Experimental Study and Response Surface Methodology Optimization of Electro-Fenton Process Reactive Orange 16 Dye Treatment

Imran Ahmad[1] · Debolina Basu[1]

Abstract

The batch mode electro-Fenton advanced oxidation process was used for Reactive Orange 16 (RO16) dye treatment. The work aimed to study and optimize the governing operational parameters (operational pH, A; initial RO16 concentration, B; electrolysis time, C; and current density, D) for decolorization and COD removal. Response surface methodology (RSM) was used for optimization. At optimum conditions (A = 3.5, B = 135 mg/L, C = 42.5 min, and D = 17.5 mA/m^2), the results show decolorization and COD removal as 72% and 61%, respectively. The Pareto graph and ANOVA results confirmed that the process was most significantly affected by current density followed by pH value and total electrolysis time; whereas the higher initial dye concentrations (> 135 mg/L) adversely affected the process efficiency. Perturbation plots support the finding of results and diagnostic plots represent a good agreement with the experimental data. The kinetic study revealed the process best represented by the pseudo 2nd order kinetics (R^2 = 0.9878); whereas, the total operational cost ($1.90 m^{-3}) indicates an economical treatment of RO16 dye-bearing Textile effluent.

Keywords Reactive orange 16 · Electro-Fenton process · Response surface methodology · Optimization · Decolorization

1 Introduction

The Textile industry plays a major role in polluting natural water resources and depletion of potable water (Akhtar et al. 2020; Gökkuş and Yıldız 2014). It is estimated that about 5×10^5 tons of dyes are consumed and 250–350 m^3 of colored wastewater is generated for every ton of finished Textile product (Arora 2014). Dyes are classified into three major groups: (1) cationic i.e. basic dyes; (2) anionic i.e. direct, acid, reactive dyes; and (3) non-ionic. As cotton fabric makes up about 50% of the total fiber consumption in the world, cotton dyeing with reactive dyes has led to an increased focus on studies of the decolorization of reactive dye-bearing Textile effluents. Furthermore, alkaline dyebath hydrolysis and lower fixation rates caused an additional waste of the reactive dyes (Sharma and Rashmi 2013). Studies have reported that during the dying process, significant amounts of dyes ($\approx$ 16–52%) fail to adhere to fabric, and are released as wastewater (Rehman et al. 2018). The reactive dyeing process has a much higher water utilization rate compared to dyeing with other types of dyes resulting generation of large volumes of highly colored spent dye baths (Sharma and Rashmi 2013). Dyes are highly toxic, carcinogenic, and mutagenic in nature (Zhang et al. 2015). Their relatively longer half-lives and poor biodegradability cause damage to the aquatic environment and human health (Lellis et al. 2019; Hassan and Christopher 2018). Dye-bearing wastewaters, discharged to a water body, can lead to reduced sunlight penetration; a lower rate of photosynthesis and dissolved oxygen levels, and an increase in turbidity (Hassan and Christopher 2018). Therefore, stringent regulations have been imposed by the statutory bodies in India and abroad, to prevent the discharge of colored effluents and to promote the installation of the on-site treatment units.

It is extremely difficult to treat reactive dyes bearing effluents by adopting conventional treatment approaches. The Reactive Orange 16 (RO16) is one such anionic dye, belonging to the azo group and soluble in the aqueous phase. These dyes impart color owing to the chromophoric groups in their molecular structures and fix the color to the fabric due to the auxotrophic groups which react with cellulose hydroxyl or amino acid functional group of wool and similar synthetic fabric (Shen and Gondal 2017; Wang et al. 2018).

✉ Imran Ahmad
  imran@mnnit.ac.in

1   Civil Engineering Department, Motilal Nehru National Institute of Technology Allahabad, Prayagraj 211004, India

The azo (N=N) group in the RO16 dye structure results in poor biodegradability leading to a lower removal efficiency of these dyes in the engineered treatment system. Failure to rely on sorption and aerobic or anaerobic biodegradation makes it necessary to identify sustainable treatment strategies for the removal of these dyes from wastewater. This indeed would be an important step undertaken to prevent the release of such recalcitrant and xenobiotic pollutants into the ecosystem. The various conventional methods that are used for dye effluent treatment include adsorption (Jesionowski et al. 2012), coagulation (Joo et al. 2007), electro-coagulation (Mook et al. 2017), reverse osmosis (Wang et al. 2018), and bio-degradation (Bouraie and Din 2016), etc. Due to the high stability and low biodegradability of dyes, these methods have several shortcomings such as incomplete degradation, high operational and chemical costs, limited applicability, and handling issues of sludge production as secondary pollutants. Table 1 summarises the comparative study of some most commonly used methods of dye treatment.

In the last few decades, advanced oxidation processes (AOPs) have been significantly developed and extensively used to treat persistent organic pollutants (POPs) present in complex industrial effluents. These processes are more efficient and effective than conventional physicochemical methods (Brillas and Martínez-Huitle 2015). In AOPs, the two methods; anodic oxidation (AO); and electro-Fenton (EF) oxidation are frequently used due to their ample *in-situ* hydroxyl radical (HO·) production. These oxidation methods have a greater redox potential ($E_o = 2.80$ V vs. SHE) and a higher capacity to oxidize pollutants (Sirés et al. 2014).

The EF oxidation method involves the coupling of the Fenton reaction with electrochemistry. The technology has been reported as promising and efficient for various POP treatments such as dyes, leachate, oily waste, medical waste, and pesticides (Gökkuş and Yıldız 2015; Nidheesh and Gandhimathi 2012). It attracted attention owing to several reasons like lower operational cost, high HO· generation, wide pollutants treatment range, efficiency adjustment (with additional HO· generation), and minimum sludge production (reproduction of Fe^{2+} from cathodic Fe^{+3} reduction) (Eq. 1):

$$Fe^{3+} + e^- \rightarrow Fe^{2+} \qquad (1)$$

The reaction mechanism of the EF process depends on the selected pollutants and used electrode materials. For the most common mechanism, hydrogen peroxide (H_2O_2) is electrochemically generated on the cathode in continuous chain mode by electrochemical reduction of atmospheric O_2 under acidic condition (Eq. 2):

$$O_2 + 2H^+ + 2e^- \rightarrow H_2O_2 \qquad (2)$$

Further, with small amount of iron catalyst (Fe^{2+}) present, H_2O_2 generates HO·, which oxidizes the complex POP into simple molecular products (Eqs. 3 and 4).

$$H_2O_2 + Fe^{2+} \rightarrow Fe^{3+} + OH^- + HO· \qquad (3)$$

$$POP + HO· \rightarrow Simple\ Molecular\ Products + CO_2 + H_2O \qquad (4)$$
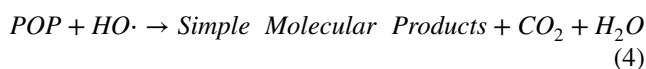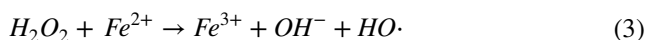
However, in the case of electrochemical reactions, the most critical aspect is the possibility of higher energy consumption due to the occurrence of parallel competitive reactions in solvent. For example, the simultaneous occurrence of oxygen evolution reaction in the solvent retards the desired oxidative reaction and causes abatement in current efficiency. Therefore, it is very important to select a suitable electrode material, for a higher oxygen evolution reaction, that can result in a higher Faradic yield. To cope with the problem, carbonaceous electrode materials are most commonly used because of their low catalytic activity for H_2O_2 decomposition (Daneshvar et al. 2008). There are various carbonaceous materials tested for H_2O_2 generation like carbon felts (Çelebi et al. 2015), carbon sponge (Özcan et al. 2008), carbon nano-tubes (Gao et al. 2015), graphite felt (Daneshvar et al. 2008), graphite paper (Fernández de Dios et al. 2015), and graphite plates (Nidheesh et al. 2014). On the flip side, another method that is also used to cut down

Table 1 Comparison of commonly used treatment technology for dye wastewater treatment

Methods	Pros/Cons	References
Physiochemical treatment	High removal efficiency/Sludge production, high operational cost, and more land area requirement	Santos et al. (2007) and Mook et al. (2017)
	Fast process/Sludge production and high operational and chemical cost	Forgacs et al. (2004) and Naim et al. (2002)
Biological treatment	Simple in operation/Low efficiency due to the persistent nature of dye to bacterial decay	Santos et al. (2007) and Forgacs et al. (2004)
Enzymatic operation	Required more knowledge for efficient application	Naim et al. (2002)
Advanced oxidation process	Higher efficiency/High operational cost	Forgacs et al. (2004) and Naim et al. (2002)
Electrochemical treatment	Environmental compatibility/Extra operational cost due to electrical energy requirement	Chen (2004) and Martínez-Huitle and Ferro (2006)

energy utilization is statistical process optimization; which reduces the number of experimental runs and operational costs (Gökkuş and Yıldız 2015).

In the study, we run the batch-mode electro-Fenton process using RO16 as the model pollutant dye. Carbon sponge anode and graphite plate cathode were used as carbonaceous electrodes because of their high electrocatalytic activity. In literature, various studies have been reported for dye treatment, but mostly they focused on parametric analysis. Here, we aimed to study the process from the fundamental operational parameter to field operational suitability by optimizing the process with the Response Surface Methodology (RSM) statistical tool. The EF process was first studied for its key operational factors effect (pH, initial RO16 concentration, total electrolysis time, and current density) on decolorization and COD removal. Further, with RSM, the multi-parameter optimization was performed. The method significantly reduces the number of experiments with a subsequent reduction in experimental cost; with the additional benefit of specifying the most significant and least/adversely affecting operational factors. The study also presents the RO16 decay kinetic and the EF process total operational costs analysis in the last section.

2 Materials and Methods

2.1 Chemicals

RO16 dye was purchased from Sigma Aldrich, USA. Sodium hydroxide, NaOH (Pellets, 98% purity), Sulfuric acid, H_2SO_4 (98% purity), and Sodium chloride, NaCl (Pellets, 99% purity) were arranged from Merck Co., Germany. Acetone, $(CH_3)_2CO$ (purity > 99%) and Hydrogen chloride, HCl (purity > 55%) were used for electrode cleaning. All the chemicals used were of analytical grade (AR).

2.2 Experimental Arrangement

The batch mode experiments were performed in a 500 mL volume undivided Pyrex glass beaker at room temperature. Porous carbon sponge anode and solid graphite plate cathode (surface area = 20 cm^2; 5 cm × 4 cm) electrodes were used with the fixed mutual spacing of 2.0 cm (Fig. 1).

For current density, DC power supply (0–30 V, 2.5 A) was used. NaCl (0.4 M) and $FeSO_4.7H_2O$ (0.5 mM) were used as supporting electrolytes and iron catalysts (Fe^{2+}), respectively. For pH value adjustment solutions of 0.1 M NaOH and 0.1 M HCl were applied. Magnetic stirrer (rpm = 300; Witeg MSH-30A 230 V Germany) and Aerator (flow rate = 1.2 L/min Sobo, Model: SB333A, China) were used for homogenous mixing and oxygen supply, respectively.

2.3 Analytical Procedures

The pH of the samples was measured by pH meter (Hack, Germany). Percentage decolorization was evaluated through a spectrophotometer (UV-3000 LAB INDIA, Germany) at λ_{max} by measuring the absorbance. Percentage COD removal was calculated as per standard methods (APHA 2005) before and after the treatment. The process performance efficiency and electrical energy consumption (EE, kWh/m^3) were calculated according to Eqs. (5) and (6) (Ahmad and Basu 2022a):
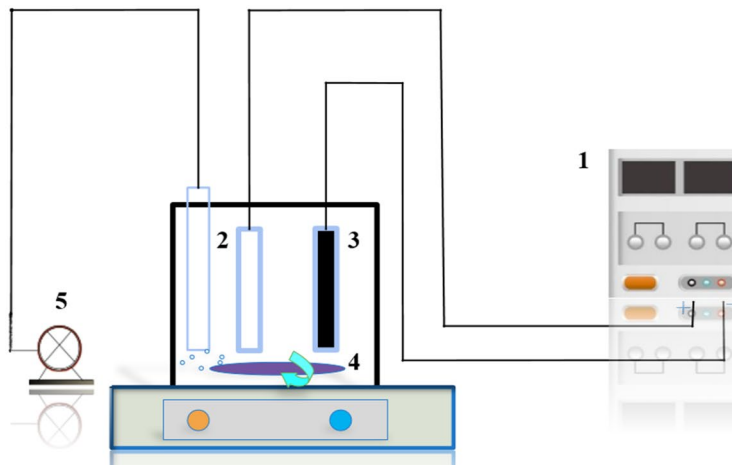
$$\%Degradation = \frac{C_o - C_t}{C_o} \tag{5}$$

$$EE(\text{kWh/m}^3) = \frac{VIt}{V_s} \tag{6}$$

where C_o and C_t are concentrations of RO16 (mg/L) before and after the treatment, respectively; V is the cell voltage

Fig. 1 Lab-scale experimental setup of the electro-Fenton process

1. DC Power Supply
2. Carbon Sponge Anode
3. Graphite Cathode
4. Magnetic Stirrer
5. Air Compressor

(V); I is the applied current; t is the electrolysis time (min); V_s (m^3) is the treated dye volume.

2.4 Design of Experiment (DOE)

Design-Expert software (version 11.1.2.0) was used for the design of the experiment (DOE). response surface methodology (RSM) was used to optimize the process parameters. The performance of the EF process was evaluated in terms of percentage removal of decolorization and COD. Four operational parameters (pH, electrolysis time, pollutant concentration, and current density) were investigated by using a central composite design (CCD). A five-level coded ($-\alpha$, -1, 0, 1, $+\alpha$) experimental design was formulated with the selected ranges of design as given in Table 2.

In CCD, three categories of experimental runs were involved i.e., center, axial, and factorial. The center runs are used to determine the experimental error; axial points ensure the model reliability; and the factorial points are the constant equidistant points from the center of the design. The total number of experimental runs was computed by using Eq. (7) (Owolabi et al. 2015):

$$\begin{aligned} &\textit{Total numbers of runs} (N) \\ &= \textit{Factorial run} + \textit{axial run} + \textit{center run} \\ &= 2^n + 2n + n_c \\ &= 2^4 + 2(4) + 6 = 30 \end{aligned} \tag{7}$$

where n, n_c are the total number of independent factors and centre points, respectively. The model suggested a total of 30 experimental run requirements for the study (16 factorials, 6 axials, and 6 centers).

2.5 Analysis of Variance (ANOVA)

With ANOVA, the validations of the model and mutual effects of operational parameters were determined. In ANOVA, the statistical parameter $p < 0.05$ determined the significant level of the polynomial equation; whereas the F-test verified the model fitting. With correlation factor (predicted and adj. R^2) the validity of model fitting was checked (Ahmad and Basu 2022b). For the study, the quadratic equation was found as the best-fitted equation for the experimental data (Table 3).

Table 2 Experimental variables with their range and levels

Process	Experimental variables	Symbol	Coded values				
			$-\alpha$	-1	0	$+1$	$+\alpha$
Electro-Fenton	pH	A	0.5	2	3.5	5	6.5
	Electrolysis time (min)	B	7.5	25	42.5	60	77.5
	Pollutant concentration (mg/L)	C	5	70	135	200	265
	Current density (mA/cm^2)	D	2.5	10	17.5	25	32.5

Table 3 ANOVA results for decolorization and COD removal

Responses	Model	Sequential P-value	Lack of Fit P-value	Adjusted R^2	Predicted R^2	
Decolorization (%)						
	Linear	0.0001	0.0065	0.5240	0.3824	
	2FI	0.9642	0.0035	0.4149	0.3802	
	Quadratic	**< 0.0001**	**0.9564**	**0.9736**	**0.9588**	**Suggested**
	Cubic	0.8623	0.8972	0.9624	0.9319	
COD removal (%)						
	Linear	< 0.0001	0.1120	0.5521	0.4189	
	2FI	0.9521	0.0682	0.4543	0.4094	
	Quadratic	**< 0.0001**	**0.9525**	**0.9092**	**0.8571**	**Suggested**
	Cubic	0.8139	0.9975	0.8775	0.9533	

The bold rows show the most accurate model with the lowest sequential P value

2.6 Pareto Analysis

The Pareto graph is used for the interpretation of significant findings of results. The graph shows the percentage effect of each operational factor on the response variables and calculated as Eq. (8) (Ahmadzadeh et al. 2017):

$$P_i = \left(\frac{b_i^2}{\Sigma b_i^2} \right) \times 100 \quad \text{(for all values of } i \neq 0) \tag{8}$$

where b_i^2 is the estimation of the square root of the operational factor and Σb_i^2 is the sum of the square root of all the operational factors.

2.7 Oxidative Degradation Kinetics

In the EF oxidation process, the rate of oxidation by free HO· radical can be given as Eq. (9):

$$r = -\frac{dq}{dt} = k_{OH}q_{OH}q_{POP} + \sum_{i}^{m} k_{Oth}q_{Oth}q_{Oth} \tag{9}$$

where q is the concentration of particular reactants and Oth represents the possible availability of other oxidants such as hydro-peroxyl radical (HOO·). A modified Eq. (10) after including the apparent rate constant (k_{app}) with HO· concentration can be re-written as (Duc et al. 2021):

$$r = -\frac{dq}{dt} = k'_{app}q_{POP} \tag{10}$$

Integrating the Eq. (10), we got the pseudo 1st order equation as:

$$ln \frac{q_o}{q} = k'_{app} \times t \tag{11}$$

where q and q_o represent the concentration at initial and after time interval t, respectively; and k'_{app} is apparent pseudo 1st order rate constant.

In the case of a pseudo 2nd-order equation reaction, the equation will be:

$$r = -\frac{dq}{dt} = k''_{app}q_{POP}^2 \tag{12}$$

Again, integration of Eq. (12) gives the final equation for pseudo 2nd-order as:

$$\frac{t}{q} = \frac{1}{k''_{app}q_e^2} + \frac{t}{q_e} \tag{13}$$

where q_e is the equilibrium concentration and k''_{app} is the apparent pseudo 2nd order rate constant. The rate constants k'_{app} and k''_{app} can be obtained by plotting ln $(q_o − q)$ versus t and t/q versus t graphs.

3 Results and Discussion

3.1 Model Fitting and Statistical Analysis

The experimental results for responses were modelled with Design-Expert software (version 11.1.2.0) and second-order polynomial equations were obtained (Eqs. 14 and 15).

$$\begin{aligned} Decolorization\ rate(\%) = {}& 71.50 + 2.51A + 7.08B − 4.42C \\ & + 11.25D − 8.23A^2 − 3.98B^2 \\ & + 4.02C^2 − 0.8542D^2 + 0.3750AB \\ & − 1.62AC − 0.2500AD + 1.50BC + 0.3750BD − 2.87CD \end{aligned} \tag{14}$$

$$\begin{aligned} COD\ Removal(\%) = {}& 60.50 + 1.59A + 7.13B − 4.88C + 12.04D \\ & − 6.97A^2 − 2.97B^2 + 5.28C^2 \\ & − 1.22D^2 + 0.1875AB − 1.56AC − 0.9375AD \\ & + 0.1875BC + 0.3125BD − 3.44CD \end{aligned} \tag{15}$$

These polynomial model equations explain the interaction of influencing parameters on decolorization and COD removal for the EF process. In the model equation, the parameters having favourable effects on the responses are represented with positive terms; while negative terms showed adversely affecting parameters. The complete CCD matrix, with the experimental results of response values of decolorization (%) and COD removal (%), is given in Table 4.

For validation of the selected 2nd-order polynomial model, ANOVA was conducted with five parameters to check the variability of data between experimental and predicted results: (1) the Prob. $> F$ to check the significant level of the model that should be < 0.0500; (2) the lack of fit test, to check the model fitting that should be > 0.0500; (3) adequate precision test to check signal-to-noise (S/N) ratio that should be ≥ 4; (4) adjusted regression coefficient (Adj. R^2); and (v) regression coefficient (R^2) that should be closer to 1 (Ahmad and Basu 2022a, b). The results showed that the response values met the model validation and accuracy criteria and can be used to anticipate the EF process performance (Table 5).

3.2 Significance of Operational Parameters

3.2.1 Pareto Graph

In the Pareto graph, the current density (D) was found to have the highest percentage contribution for the decolorization (%) and COD removal (%) with a total of 40.8% and 45.06%, respectively. The interaction effect of pH (A2) and electrolysis time (B) has a significant contribution to decolorization (38%) and COD removal (30.9%) showing

Table 4 The design matrix, predicted and observed values for the response variables

| Run | Space type | Independent experimental variables | | | | Response values | | | |
| | | A | B | C | D | Decolorization rate (%) | | COD removal (%) | |
						Predicted	Observed	Predicted	Observed
1	Centre	3.5	42.5	135	17.5	71.50	70	60.50	55
2	Factorial	5.0	25	200	25	55.21	55	48.17	48
3	Factorial	2.0	60	200	10	58.88	60	48.46	52
4	Axial	3.5	42.5	265	17.5	78.75	78	71.88	68
5	Factorial	2.0	25	70	25	74.04	75	67.17	70
6	Axial	3.5	42.5	135	2.5	45.58	45	31.54	30
7	Factorial	5.0	25	200	10	39.71	40	33.46	35
8	Factorial	5.0	60	200	10	56.88	55	47.83	45
9	Axial	3.5	42.5	135	32.5	90.58	92	79.71	81
10	Factorial	5.0	60	70	25	88.71	86	83.17	80
11	Axial	6.5	42.5	135	17.5	38.58	40	32.88	35
12	Axial	3.5	42.5	5	17.5	96.42	98	91.38	95
13	Centre	3.5	42.5	135	17.5	71.50	75	60.50	68
14	Centre	3.5	42.5	135	17.5	71.50	75	60.50	68
15	Factorial	2.0	25	200	25	59.71	60	53.29	55
16	Axial	0.5	42.5	135	17.5	38.58	38	32.38	30
17	Factorial	2.0	25	200	10	43.21	45	34.83	38
18	Factorial	5.0	25	70	10	49.04	50	39.83	42
19	Factorial	5.0	60	200	25	73.88	75	63.79	67
20	Axial	3.5	77.5	135	17.5	69.75	72	62.88	65
21	Factorial	2.0	60	70	25	85.21	85	81.29	80
22	Centre	3.5	42.5	135	17.5	71.50	65	60.50	50
23	Factorial	2.0	25	70	10	46.04	45	34.96	32
24	Axial	3.5	7.5	135	17.5	41.42	40	34.38	32
25	Factorial	5.0	60	70	10	60.21	60	53.46	52
26	Centre	3.5	42.5	135	17.5	71.50	72	60.50	61
27	Centre	3.5	42.5	135	17.5	71.50	72	60.50	61
28	Factorial	2.0	60	200	25	76.88	75	68.17	66
29	Factorial	2.0	60	70	10	55.71	55	47.83	48
30	Factorial	5.0	25	70	25	76.04	75	68.29	65

a contributory effect on the process performance. For both responses, the total substantial contributions for the above three factors were observed as 65.76% and 69.85%, respectively. Factors A, C, CD, and B2 have shown less significant contributors whereas AB, AC, AD, BC, BD, and D2 were observed not to contribute any significant effect on the process performance (Fig. 2). The observed result for current density was supported by Daneshvar et al. (2007) work on Acid Yellow 23 removals; whereas the pH and electrolysis time contribution effects were also reported by Bashir et al. (2019) and GilPavas et al. (2019) work on palm oil mill effluent and Textile wastewater treatment.

3.2.2 Perturbation Plots

For comparing the effect of the different input factors on the response values *at any particular point* of design space, perturbation plots were drawn. These plots interpreted the process performance for variation of an operational factor within the operational range, with other factors as constant. The sensitivity of response for any operational factor can be judged by the steepness of the curvature of the plot. In our study, two perturbation charts were plotted at the optimal point of design space (A = 3.5; B = 42.5 min; C = 135 mg/L; and D = 17.5 mA/cm^2) for

Table 5 ANOVA result of the EF process

Source	SoS#	df*	MoS$	F-Value	Prob. > F	Remarks
Decolorization (%)						
Model	7878.62	14	562.76	77.27	< 0.0001	Significant
Lack of Fit	39.75	10	3.97	0.2860	0.9564	Not significant
Pure Error	69.50	5	13.90			
Cor. Total	7987.87	29				
Adequate Precision	30.306					
R^2	0.9863					
Adj.R^2	0.9736					
COD Removal (%)						
Model	8179.72	14	584.27	21.74	< 0.0001	Significant
Lack of Fit	149.58	10	14.96	0.2950	0.9525	Not significant
Pure error	253.50	5	50.70			
Cor Total	8582.80	29				
Adequate Precision	16.323					
R^2	0.9530					
Adj.R^2	0.9092					

SoS# = Sum of the square; df* = Degree of freedom; MoS$ = Mean of square

Fig. 2 Pareto graph for operational parameters
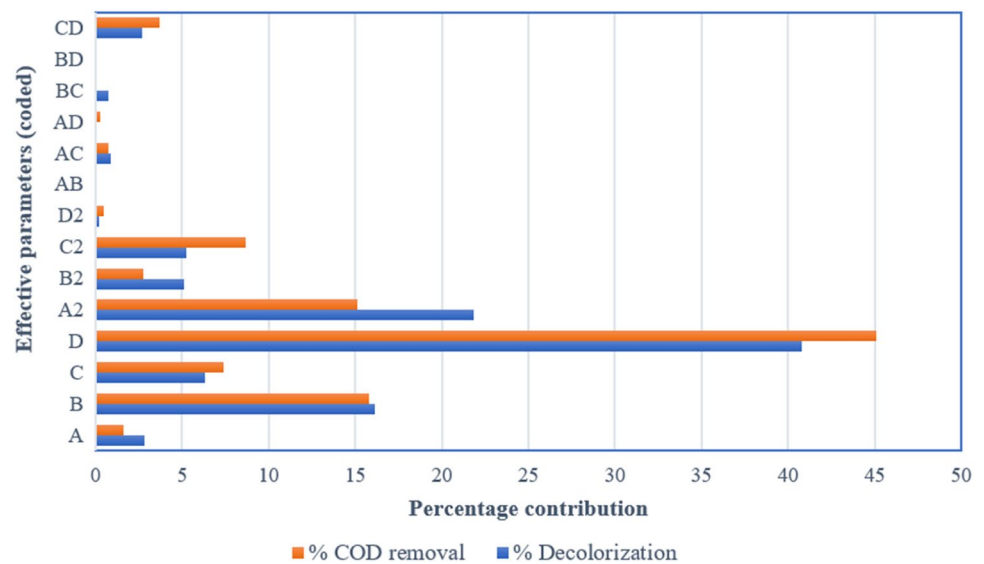
the response values of decolorization and COD removal (Fig. 3). The steepness of plots showed that the process was most significantly affected by current density (D), and least by dye concentration (C) for both observed responses of decolorization and COD removal. The results were supported by Akhtar et al. (2020) work on Congo Red dye removal by the electro-coagulation process.

3.3 Parametric Discussion

3.3.1 Effect of pH Value

At high dye concentrations (200 mg/L), lower pH values showed enhancement in decolorization from 62.3 to 73.5%, which gradually reduced to 63% as the pH > 3.5. At lower dye concentration (70 mg/L), the decolorization initially
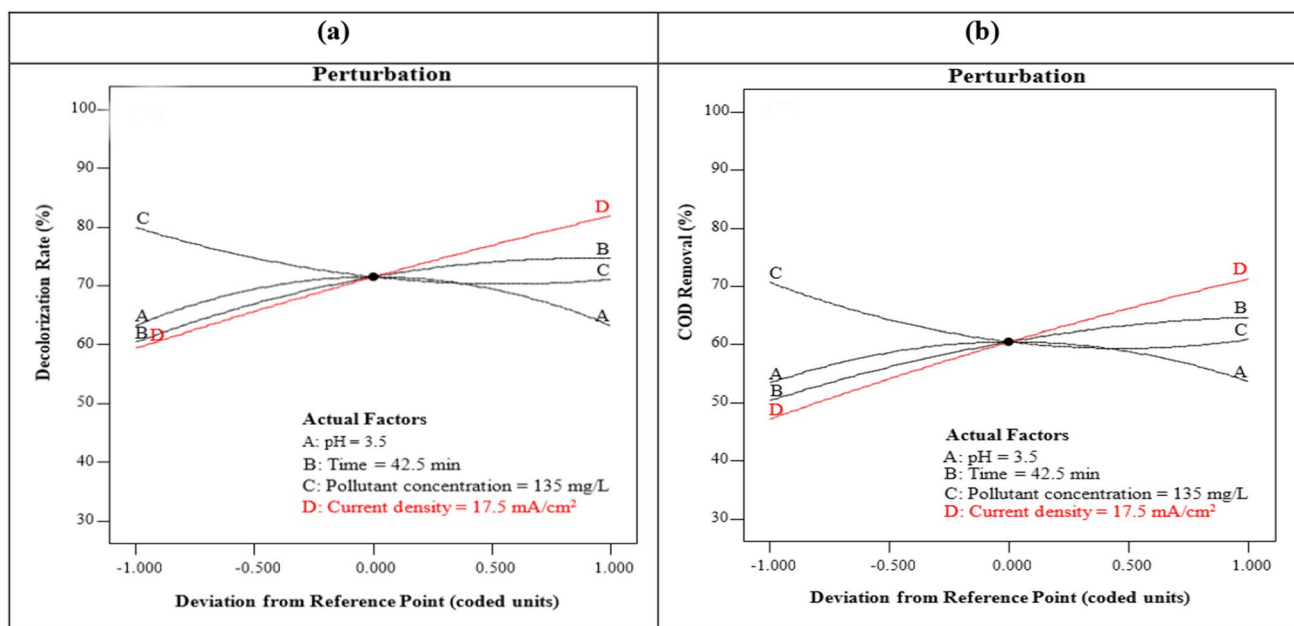
Fig. 3 Perturbation plots for **a** demineralization (%); and **b** COD removal (%)

increased from 42.3 to 75% and further decreased to 73% for pH > 3.5 (Fig. 4b). Similar trends were also obtained for COD removal (%) with a reduction in the result of approximately 10% and 1% for high (200 mg/L) and lower dye concentration (70 mg/L) for pH > 3.5, respectively (Fig. 5b). The obtained result was supported by the result reported by Wang et al. (2014) for Methylene Blue dye treatment. In general, a pH in the range of 2.5–3.5 is often reported to be more favorable for the removal of dyes in the EF process (Ahmad and Basu 2023). A higher pH leads to more ferric ions (Fe^{2+}) precipitation in aqueous solution; whereas natural or lower pH causes the accumulation of hydroxyl ions by H^+ ions (Hodaifa et al. 2013; Nieto et al. 2011). In both of the cases, an overall decrement in the oxidative power of the EF process occurred.

3.3.2 Effect of Current Density

From the 3D plots of the current density effect on decolorization and COD removal, it can be said that there was an overall increment in dye degradation with an increase in current density. The possible reason could be that at higher voltage more free electrons boost the rate of Fe^{+2} regeneration (Eq. 1) which subsequently increases the free HO· and H_2O_2 production (Moreira et al. 2017).

Figures 4c) and 5c explain the effect of current density on decolorization and COD removal, respectively. The decolorization showed an incensement with an increase in current density, independent of the pH value. However, this effect was less significant for COD removal. At a higher

pH value (> 3.5), an increment in current density from 10 to 25 mA/cm² increases the decolorization (%) from 50.53 to 73.69%; while a lower pH value (< 3.5), it was 31.61 to 73.69%. Wang et al. (2014) also reported a similar increment in color removal efficiency from 56.1 to 70.8%, for an increase in current density from 11 to 80 A/m² in their EF process of real Textile wastewater treatment.

3.3.3 Effect of Initial Dye Concentration

The EF process effect for dye concentration has found to work better at lower values (Figs. 4d, f and 5d, f)). At higher dye concentrations, the higher formation of intermediate products reduced the amount of HO· radicals that attack directly the targeted dye pollutants, decreasing overall efficiency (García-Rodríguez et al. 2016). Also, at higher dye concentrations, the consumption of free radical HO· increases more than its production, leading to a deficiency of available free radicals (HO·) (Yousefi et al. 2018).

3.3.4 Effect of Electrolysis Time

The results on process performance for the effect of electrolysis time are shown in Figs. 4 and 5. It was found that an increment in total electrolysis time favoured the process efficiency. Figure 4e and 5e showed that for a constant current density, the decolorization increased from 70.36% (25 min) to 85.16% (60 min) and COD removal increased from 60% (25 min) to 75.85% (60 min). The possible reason could be an increment in electrolysis time caused more
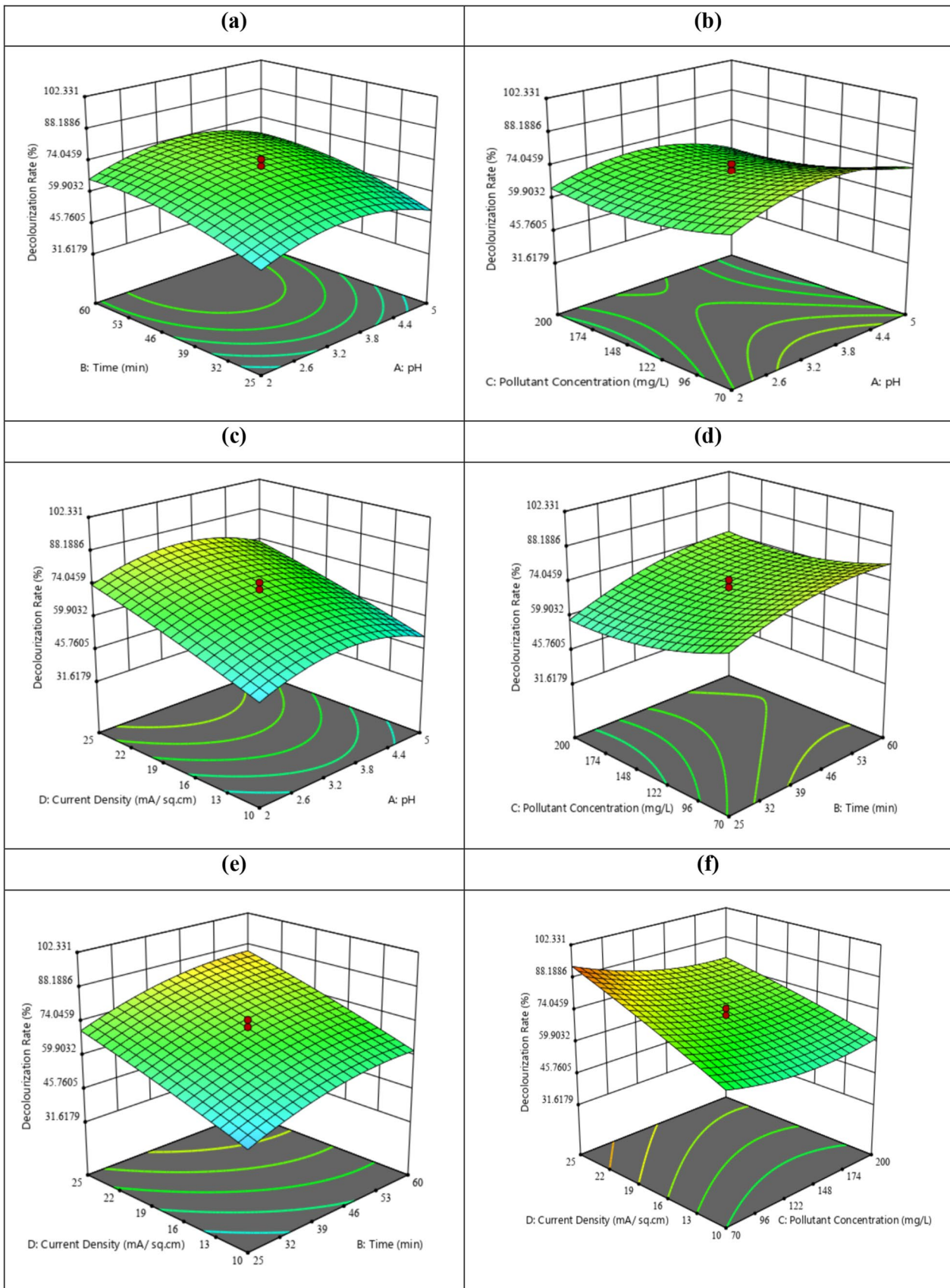
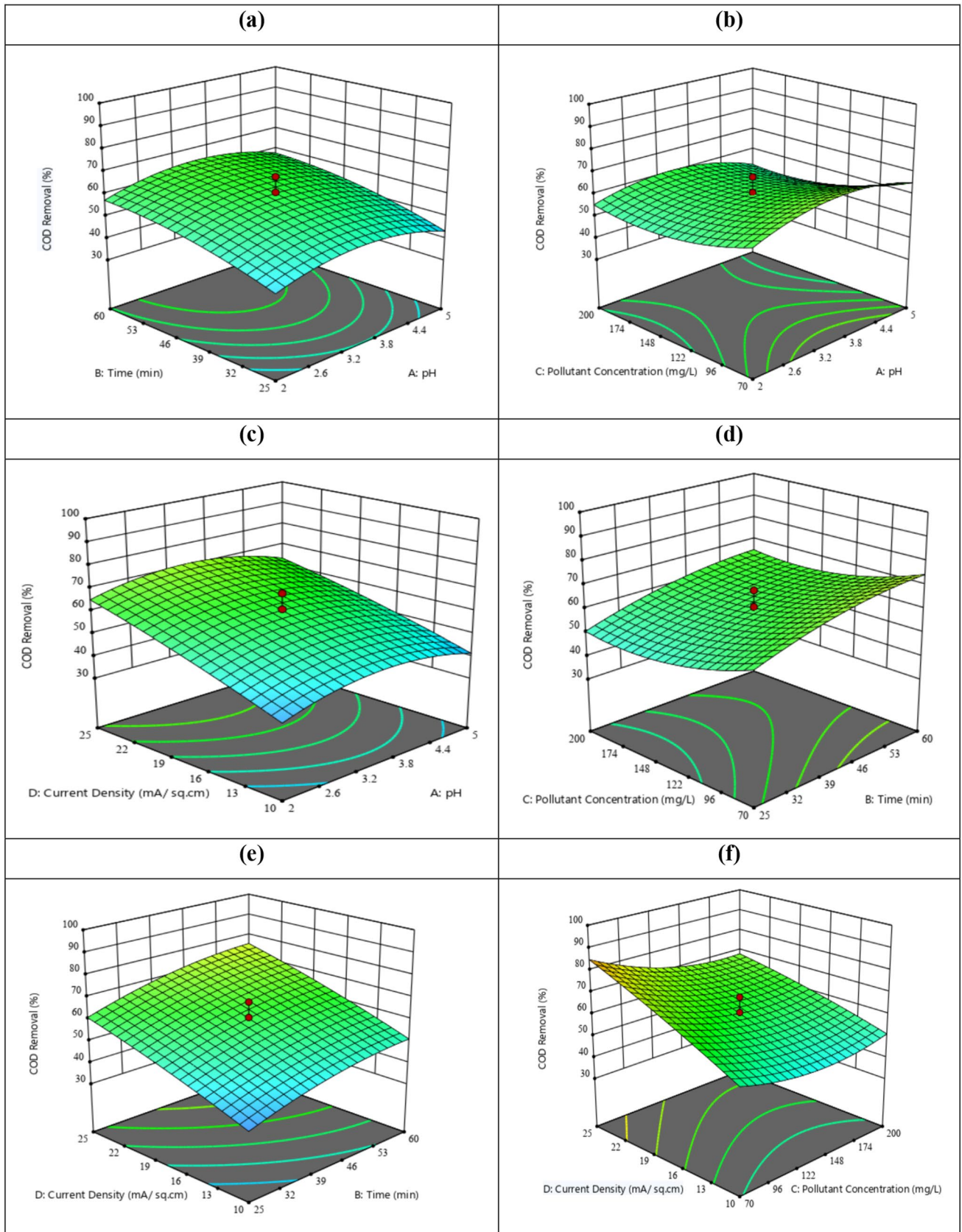**Fig. 4** Operating factors interaction effect on decolorization (%)

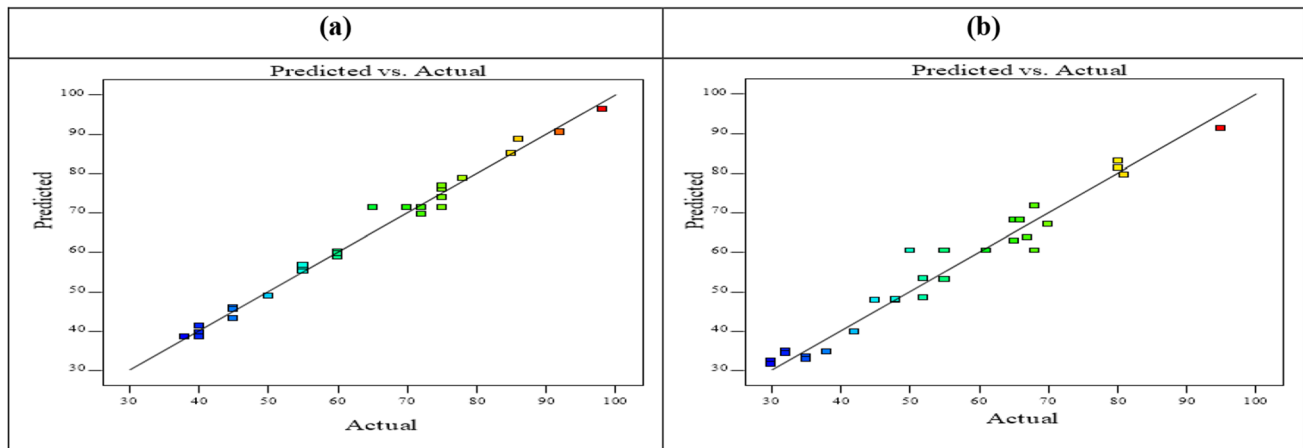**Fig. 5** Operating factors interaction effect on COD (%) removal

Fig. 6 Predicted versus actual values plot for **a** decolorization (%) and **b** COD removal (%)

HO· production that caused more H_2O_2 decomposition subsequently (Özcan et al. 2008). For a variable pH range, this increment was up to a pH of 3.5, after that graph showed a reverse trend (Figs. 4a and 5a). This was due to the possible reason of Fe^{2+} precipitation in the aqueous solution, that consequently decreased HO· production and reduced the treatment efficiency as discussed earlier in Sect. 3.3.1.

3.4 Statistical Model Validation

The result showed a good agreement between predicted and experimental values Fig. 6 a, b. Further, diagnostic curves for hypotheses of mathematical models were drawn to check the model adequacy Fig. 7. In Fig. 7a and b, colored points showed the residuals, and their closeness to the bisector line confirmed the normality of residuals (Dehghan et al. 2018). In Fig. 7c–f the plots of residuals showed a random distribution without any particular trend line confirming the 2nd-order model suitability (Yousefi et al. 2018). Therefore, the plots for residuals are normal and acceptable for response values prediction.

4 Kinetic Study

Pseudo 1st and 2nd order kinetic model was used to test the best fitted equation for experimental data. The kinetic constants values for 1st and 2nd order kinetic models were obtained at different RO16 dye concentrations (Table 6). The result showed a better fitment of experimental data

with the pseudo 2nd order model because of the higher regression coefficients (R^2) values. Also, with higher RO16 concentration, the decreasing R^2 value represents a possible increment of competitive reactions among the HO· and other oxidative by products (Mansour et al. 2015).

Figure 8 represents the relationship between rates of reaction (k_{app}' and k_{app}'') with RO 16 dye concentration (q_{POP}). Accordingly, the kinetic models for RO16 dye degradation were given by Eqs. (16) and (17):

Pseudo 1st order model:

$$r = -\frac{dq}{dt} = 0.0094q_{POP} \tag{16}$$

Pseudo 2nd order model:

$$r = -\frac{dq}{dt} = 0.0806q_{POP}^2 \tag{17}$$

Therefore, the rate of the pseudo 2nd order model was 8.57 times faster than the pseudo 1st order model.

5 Cost Analysis

The operational cost (OC) plays a major constraint on the application suitability of any treatment technology. It may include the cost of electrical energy (EE), chemical, electrode consumption (EC), etc. For the current study, the total OC at optimum condition was calculated as \$0.54 m^{-3} for the commercial Indian electric price rate of \$0.14 kWh^{-1}. The chemical cost was \$1.23 m^{-3} (\$2.58 kg^{-1} for H_2SO_4;
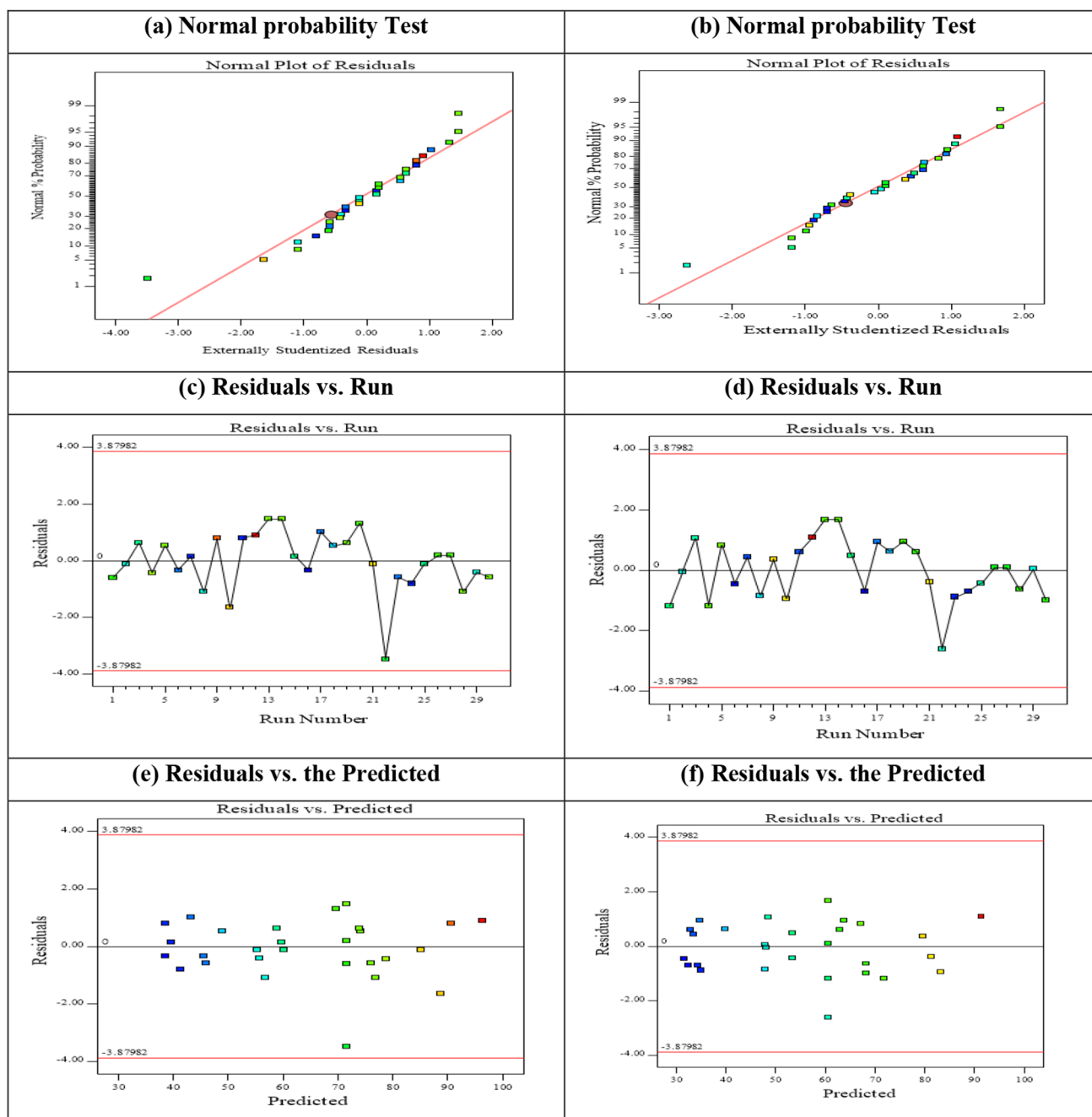
Fig. 7 Diagnostics plots for decolorization and COD removal: **a** and **b** for normal probability test, **c** and **d** for residuals versus run number, and (**e** and **f**) for residuals versus predicted values

$2.06 kg^{-1} for NaCl; $3.6 kg^{-1} for NaOH; and $0.05 kg^{-1} for $FeSO_4.7H_2O$) which was about 66% of the total cost. In Zheng and Lefebvre (2019) study, they reported that the total OC for the majority of the homogeneous EF process can be distributed as electrical energy (29%), chemical cost

(64%), and remaining (7%) cost for others such as electrode consumption (EC) cost. Using this study result, the other cost (EC) for the electrode materials consumption was calculated and overall results are reported in Table 7. The result concludes that the EF process can be used as a substitution

Table 6 Kinetic constants at different initial RO16 dye concentration (A = 3.5, C = 45 min, D = 17.5 mA/cm^2)

Reactive orange 16 concentration (mg/L)	Pseudo 1st order		Pseudo 2nd order	
	k'_{app}	R^2	k''_{app}	R^2
200	0.0265	0.9641	0.2681	0.9531
400	0.0205	0.9804	0.1972	0.9623
600	0.0179	0.8913	0.1098	0.9698
800	0.0110	0.8523	0.0981	0.9912
1000	0.0094	0.8817	0.0806	0.9882
1200	0.0035	0.9579	0.0809	0.9723

method over other processes such as electro-coagulation that cost highly because of huge chemical consumption.

6 Conclusion

A batch-mode experimental study and optimization of the EF process was done with Response surface methodology (RSM). For the selected operational parameters, the optimized result was obtained as pH (A) = 3.5, electrolysis time (B) = 42.5 min, initial dye concentration (C) = 135 mg/L, and current density (D) = 17.5 mA/cm^2, with decolorization and COD removal as 72% and 61% respectively. For the EF process efficiency, current density (D) affects the process most; whereas the higher RO16 dye concentration (> 135 mg/L) adversely affects the process. The ANOVA result showed 2nd order polynomial model suitability for decolorization ($R^2 = 0.9863$) and COD removal ($R^2 = 0.9530$) and diagnostic plots validated the developed statistical models. The Pareto graph ordered the effect of operational parameters as: current density > pH > electrolysis time > initial RO16 dye concentration. Also, the Perturbation plots support the result at optimized conditions. The kinetic study was best suited by 2nd order polynomial model ($R^2 = 0.9878$). Also, the overall cost ($1.9 m^{-3}) at the optimized conditions favoured an economical treatment of dye pollutants. Future research can be aimed at using other optimization tools (Taguchi design and Artificial Neural Networks) to further analyze and compare the result for the best optimization tool selection and to better understand the lab-scale EF process experimental design, particularly adapted for the economical treatment of Textile Industrial pollutants.
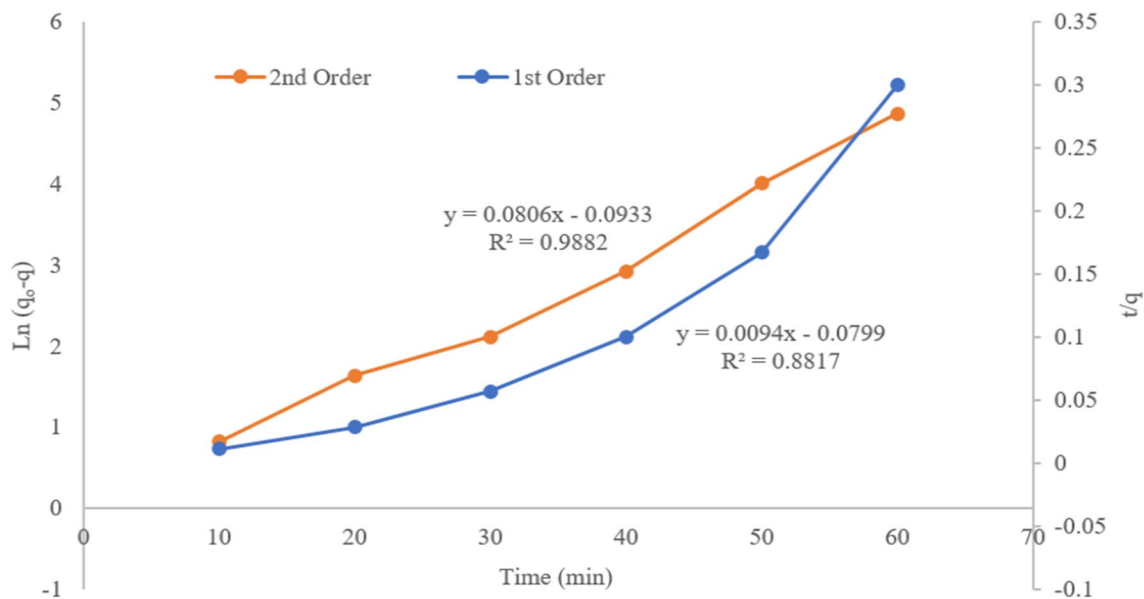
Fig. 8 Pseudo 2nd order kinetic model for RO16 degradation (A = 3.5; B = 1000 mg/L; D = 17.5 mA/cm^2)

Table 7 Various operational costs analysis

Pollutant	pH	Current density (mA/cm^2)	EE cost ($/m^3)	Chemical cost ($/m^3)	EC cost ($/m^3)	OC ($/m^3)
RO16	3.5	17.5	0.54	1.23	0.13	1.90

Declarations

Conflict of interest The authors declare no conflict of interest.

References

Ahmad I, Basu D (2022a) Taguchi L16 (44) orthogonal array-based study and thermodynamics analysis for electro-Fenton process treatment of Textile industrial dye. Chem Prod Process Model. https://doi.org/10.1515/cppm-2022-0045

Ahmad I, Basu D (2022b) Application of the central composite design and Taguchi method for the optimization of the electro-Fenton process treatment of Textile industrial dye. Indian J Environ Prot 42(13):1448–1454

Ahmad I, Basu D (2023) Comparative study on the role of single-and double-cathode in electro-Fenton process for treatment of Reactive Orange 16 dye bearing wastewaters. Int J Environ Anal Chem 16:1–21. https://doi.org/10.1080/03067319.2023.2264786

Ahmadzadeh S, Asadipour A, Pournamdari M, Behnam B, Rahimi HR, Dolatabadi M (2017) Removal of ciprofloxacin from hospital wastewater using electrocoagulation technique by aluminum electrode: Optimization and modelling through response surface methodology. Process Saf Environ Prot 109:538–547. https://doi.org/10.1016/j.psep.2017.04.026

Akhtar A, Aslam Z, Asghar A, Bello MM, Raman AAA (2020) Electrocoagulation of Congo red dye-containing wastewater: optimization of operational parameters and process mechanism. J Environ Chem Eng 8(5):104055. https://doi.org/10.1016/j.jece.2020.104055

APHA (2005) Standard methods for the examination of water and wastewater, 21st edn. American Public Health Association/American Water Works Association/Water Environment Federation, Washington, DC

Arora S (2014) textile dye: its impact on environment and its treatment. J Biorem Biodegrad 5(3):6199. https://doi.org/10.4172/2155-6199.1000e146

Bashir MJ, Lim JH, Abu Amr SS, Wong LP, Sim YL (2019) Post treatment of palm oil mill effluent using electro-coagulation-peroxidation (ECP) technique. J Clean Prod 208:716–727. https://doi.org/10.1016/j.jclepro.2018.10.073

Brillas E, Martínez-Huitle CA (2015) Decontamination of wastewaters containing synthetic organic dyes by electrochemical methods. an updated review. Appl Catal B 166–167:603–643. https://doi.org/10.1016/j.apcatb.2014.11.016

Çelebi MS, Oturan N, Zazou H, Hamdani M, Oturan MA (2015) Electrochemical oxidation of carbaryl on platinum and boron-doped diamond anodes using electro-fenton technology. Sep Purif Technol 156:996–1002. https://doi.org/10.1016/j.seppur.2015.07.025

Chen G (2004) Electrochemical technologies in wastewater treatment. Sep Purif Technol 38(1):11–41. https://doi.org/10.1016/j.seppur.2003.10.006

Daneshvar N, Khataee AR, Amani Ghadim AR, Rasoulifard MH (2007) Decolorization of C.I. Acid Yellow 23 solution by electrocoagulation process: investigation of operational parameters and evaluation of specific electrical energy consumption (SEEC). J Hazard Mater 148(3):566–572. https://doi.org/10.1016/j.jhazmat.2007.03.028

Daneshvar N, Aber S, Vatanpour V, Rasoulifard MH (2008) Electro-fenton treatment of dye solution containing orange ii: influence of operational parameters. J Electroanal Chem 615(2):165–174. https://doi.org/10.1016/j.jelechem.2007.12.005

Dehghan S, Rezaei Kalantary R, Nazari S, Moradi M, Rastegar A, Shirzad Siboni M (2018) Optimization of dimethyl phthalate degradation parameters using zero-valent iron nanoparticles by response surface methodology: determination of degradation intermediate products and process pathway. J Mazandaran Univ Med Sci 27(157):194–216

dos Santos AB, Cervantes FJ, van Lier JB (2007) Review paper on current technologies for decolorisation of textile wastewaters: perspectives for anaerobic biotechnology. Biores Technol 98(12):2369–2385. https://doi.org/10.1016/j.biortech.2006.11.013

Duc DDN, Huy HPQ, Xuan HN, Tan PN (2021) The treatment of real dyeing wastewater by the electro-Fenton process using drinking water treatment sludge as a catalyst. R Soc Chem 11(44):27443–27452. https://doi.org/10.1039/D1RA04049A

El Bouraie M, El Din WS (2016) Biodegradation of reactive black 5 by aeromonas hydrophila strain isolated from dye-contaminated textile wastewater. Sustainable Environment Research 26(5):209–216. https://doi.org/10.1016/j.serj.2016.04.014

Fernández de Dios MÁ, Rosales E, Fernández-Fernández M, Pazos M, Sanromán MÁ (2015) Degradation of organic pollutants by heterogeneous electro-fenton process using mn-alginate composite. J Chem Technol Biotechnol 90(8):1439–1447. https://doi.org/10.1002/jctb.4446

Forgacs E, Cserháti T, Oros G (2004) Removal of synthetic dyes from wastewaters: a review. Environ Int 30(7):953–971. https://doi.org/10.1016/j.envint.2004.02.001

Gao G, Zhang Q, Hao Z, Vecitis CD (2015) Carbon nanotube membrane stack for flow-through sequential regenerative electro-fenton. Environ Sci Technol 49(4):2375–2383. https://doi.org/10.1021/es505679e

García-Rodríguez O, Bañuelos JA, El-Ghenymy A, Godínez LA, Brillas E, Rodríguez-Valadez FJ (2016) Use of a carbon felt-iron oxide air-diffusion cathode for the mineralization of malachite green dye by heterogeneous electro-fenton and UVA photoelectro-fenton processes. J Electroanal Chem 767:40–48. https://doi.org/10.1016/j.jelechem.2016.01.035

GilPavas E, Dobrosz-Gómez I, Gómez-García MÁ (2019) Optimization and toxicity assessment of a combined electrocoagulation, H_2O_2/Fe^{2+}/UV and activated carbon adsorption for textile wastewater treatment. Sci Total Environ 651:551–560. https://doi.org/10.1016/j.scitotenv.2018.09.125

Gökkuş Ö, Yıldız YS (2014) Investigation of the effect of process parameters on the coagulation-flocculation treatment of Textile wastewater using the Taguchi experimental method. Fresenius Environ Bull 23(2):463–470

Gökkuş Ö, Yıldız YŞ (2015) Application of electrocoagulation for treatment of medical waste sterilization plant wastewater and optimization of the experimental conditions. Clean Technol Environ Policy 17:1717–1725. https://doi.org/10.1007/s10098-014-0897-2

Hassan MM, Christopher MC (2018) A critical review on recent advancements of the removal of reactive dyes from dyehouse effluent by ion-exchange adsorbents. Chemosphere 209:201–219. https://doi.org/10.1016/j.chemosphere.2018.06.043

Hodaifa G, Ochando-Pulido JM, Rodriguez-Vives S, Martinez-Ferez A (2013) Optimization of continuous reactor at pilot scale for olive-oil mill wastewater treatment by fenton-like process. Chem Eng J 220:117–124. https://doi.org/10.1016/j.cej.2013.01.065

Jesionowski T, Nowacka M, Ciesielczyk F (2012) Electrokinetic properties of hybrid pigments obtained via adsorption of organic dyes on the silica support. Pigm Resin Technol 41(1):9–19. https://doi.org/10.1108/03699421211192235

Joo DJ, Shin WS, Choi JH, Choi SJ, Kim MC, Han MH, Ha TW, Kim YH (2007) Decolorization of reactive dyes using inorganic

coagulants and synthetic polymer. Dyes Pigm 73(1):59–64. https://doi.org/10.1016/j.dyepig.2005.10.011

Lellis B, Fávaro-Polonio CZ, Pamphile JA, Polonio JC (2019) Effects of textile dyes on health and the environment and bioremediation potential of living organisms. Biotechnol Res Innov 3(2):275–290. https://doi.org/10.1016/j.biori.2019.09.001

Mansour D, Fourcade F, Soutrel I, Hauchard D, Bellakhal N, Amrane A (2015) Mineralization of synthetic and industrial pharmaceutical effluent containing trimethoprim by combining electro-fenton and activated sludge treatment. J Taiwan Inst Chem Eng 53:58–67. https://doi.org/10.1016/j.jtice.2015.02.022

Martínez-Huitle CA, Ferro S (2006) Electrochemical oxidation of organic pollutants for the wastewater treatment: direct and indirect processes. Chem Soc Rev 35(12):1324–1340. https://doi.org/10.1039/B517632H

Mook WT, Ajeel MA, Aroua MK, Szlachta M (2017) The application of iron mesh double layer as anode for the electrochemical treatment of reactive black 5 dye. J Environ Sci (China) 54:184–195. https://doi.org/10.1016/j.jes.2016.02.003

Moreira FC, Boaventura RAR, Brillas E, Vilar VJP (2017) Electrochemical advanced oxidation processes: a review on their application to synthetic and real wastewaters. Appl Catal B 202:217–261. https://doi.org/10.1016/j.apcatb.2016.08.037

Naim MM, El Abd YM (2002) Removal and recovery of dyestuffs from dyeing wastewaters. Sep Purif Methods 31(1):171–228. https://doi.org/10.1081/SPM-120006116

Nidheesh PV, Gandhimathi R (2012) Trends in electro-fenton process for water and wastewater treatment: an overview. Desalination 299:1–15. https://doi.org/10.1016/j.desal.2012.05.011

Nidheesh PV, Gandhimathi R, Velmathi S, Sanjini NS (2014) Magnetite as a heterogeneous electro fenton catalyst for the removal of rhodamine b from aqueous solution. RSC Adv 4(11):5698–5708. https://doi.org/10.1039/C3RA46969G

Nieto LM, Hodaifa G, Rodríguez S, Giménez JA, Ochando J (2011) Degradation of organic matter in olive-oil mill wastewater through homogeneous fenton-like reaction. Chem Eng J 173(2):503–510. https://doi.org/10.1016/j.cej.2011.08.022

Owolabi RU, Usman MA, Kehinde AJ (2015) Modelling and optimization of process variables for the solution polymerization of styrene using response surface methodology. J King Saud Univ Eng Sci 30(1):22–30. https://doi.org/10.1016/j.jksues.2015.12.005

Özcan A, Şahin Y, Savaş KA, Oturan MA (2008) Carbon sponge as a new cathode material for the electro-fenton process: comparison with carbon felt cathode and application to degradation of synthetic dye basic blue 3 in aqueous medium. J Electroanal Chem 616(1–2):71–78. https://doi.org/10.1016/j.jelechem.2008.01.002

Rehman K, Shahzad T, Sahar A, Hussain S, Mahmood F, Siddique MH, Siddique MA, Rashid MI (2018) Effect of reactive black 5 azo dye on soil processes related to C and N cycling. Peer J 5:1–14. https://doi.org/10.7717/peerj.4802

Sharma SK, Rashmi S (2013) Wastewater reuse and management. Springer, Befrlin, pp 1–500

Shen K, Gondal MA (2017) Removal of hazardous rhodamine dye from water by adsorption onto exhausted coffee ground. J Saudi Chem Soc 21:120–127. https://doi.org/10.1016/j.jscs.2013.11.005

Sirés I, Brillas E, Oturan MA, Rodrigo MA, Panizza M (2014) Electrochemical advanced oxidation processes: today and tomorrow. A review. Environ Sci Pollut Res 21(14):8336–67. https://doi.org/10.1007/s11356-014-2783-1

Wang Q, Tian S, Ning P (2014) Ferrocene-catalyzed heterogeneous fenton-like degradation of methylene blue: influence of initial solution pH. Ind Eng Chem Res 53(15):6334–6340. https://doi.org/10.1021/ie500115j

Wang J, Zhang T, Mei Y, Pan B (2018) Treatment of reverse-osmosis concentrate of printing and dyeing wastewater by electro-oxidation process with controlled oxidation-reduction potential (ORP). Chemosphere 201:621–626. https://doi.org/10.1016/j.chemosphere.2018.03.051

Yousefi Z, Zafarzadeh A, Ghezel A (2018) Application of taguchi's experimental design method for optimization of acid red 18 removal by electrochemical oxidation process. Environ Health Eng Manag J 5(4):241–248. https://doi.org/10.15171/EHEM.2018.32

Zhang D, Yin J, Zhao J, Zhu H, Wang C (2015) Adsorption and removal of tetracycline from water by petroleum coke-derived highly porous activated carbon. J Environ Chem Eng 3(3):1504–1512. https://doi.org/10.1016/j.jece.2015.05.014

Zheng X, Lefebvre O (2019) Sequential 'electrochemical peroxidation electro-fenton' process for anaerobic sludge treatment. Water Res 154:277–286. https://doi.org/10.1016/j.watres.2019.01.063